Optical excitation of single- and multi-mode magnetization precession in Galfenol nanolayers

A. V. Scherbakov,[1,2] A. P. Danilov,[1] F. Godejohann,[1] T. L. Linnik,[3] B. A. Glavin,[3] L. A. Shelukhin,[2] D. P. Pattnaik,[4] M. Wang,[4] A. W. Rushforth,[4] D. R. Yakovlev,[1,2] A. V. Akimov,[4] and M. Bayer[1,2]

[1]*Experimentelle Physik 2, Technische Universität Dortmund, D-44227 Dortmund, Germany*
[2]*Ioffe Institute, Russian Academy of Science, 194021 St.Petersburg, Russia*
[3]*Department of Theoretical Physics, V.E. Lashkaryov Institute of Semiconductor Physics, 03028 Kyiv, Ukraine*
[4]*School of Physics and Astronomy, University of Nottingham, Nottingham NG7 2RD, UK*

We demonstrate a variety of precessional responses of the magnetization to ultrafast optical excitation in nanolayers of Galfenol (Fe,Ga), which is a ferromagnetic material with large saturation magnetization and enhanced magnetostriction. The particular properties of Galfenol, including cubic magnetic anisotropy and weak damping, allow us to detect up to 6 magnon modes in a 120nm layer, and a single mode with effective damping $\alpha_{eff} = 0.005$ and frequency up to 100 GHz in a 4-nm layer. This is the highest frequency observed to date in time-resolved experiments with metallic ferromagnets. We predict that detection of magnetisation precession approaching THz frequencies should be possible with Galfenol nanolayers.

Within the last decade magnetization precession has become an actively exploited tool in nanoscale magnetism. The precessing magnetization of a ferromagnet is an effective, tunable and nanoscopic source of microwave signals. Generation of microwave magnetic fields by precessing magnetization is already implemented in magnetic storage technology such as microwave assisted magnetic recording (MAMR) [1] by means of spin-torque nano-oscillators [2]. Spin waves or magnons, i.e. the waves of precessing magnetization, are information carriers and encoders in magnonics [3] aimed to substitute conventional CMOS technology. The precessing magnetization is also an effective tool to generate a pure spin current in a nonmagnetic material by means of spin pumping [4].

The common way to excite magnetization precession in a ferromagnet is the technique of ferromagnetic resonance (FMR). A monochromatic microwave magnetic field drives the magnetization precession, the frequency of which is tuned into resonance with the microwaves by an external magnetic field. This technique, which can provide comprehensive information about the main precession parameters, is not adaptable for practical use with nanostructures due to the need of bulky electromagnetic resonators and waveguides. An alternative approach is broad-band excitation induced by dc-current [5], picosecond magnetic field pulses [6], ultrashort laser pulses [7] and strain pulses [8]. In those cases the parameters of the excited magnetization precession, i.e. the spectral content, lifetime, spatial distribution and their dependences on external magnetic field, are determined by the properties of the ferromagnetic material and the design of the nanostructure [9]. The ability to control these dynamical parameters is of crucial importance for nanoscale magnetic applications. For practical use, an ideal combination of dynamical parameters includes a tunable and narrow spectral band in the GHz and THz frequency ranges; large saturation magnetization and high precession amplitude for high microwave power; and ultrafast triggering for high-frequency modulation. Achieving this combination has been an unmet challenge until now. High precession frequency, $f \gg 10$ GHz, can be reached by using ferrimagnetic materials [10, 11], but the weak net magnetization limits their functionality. In the case of metallic ferromagnets with large net magnetization, the direct way to achieve high frequency precession is to apply a strong external magnetic field, $\mathbf{B}$, which, however, drastically decreases the precession amplitude. Earlier experiments on the excitation of magnetization precession in metallic ferromagnets by femtosecond optical pulses [7, 12–18], i.e. the fastest method of launching precession, report also high values of the effective damping coefficient $\alpha_{eff} = (2\pi\tau f)^{-1} > 0.01$ (τ is the precession decay time). Thus, the excitation and detection of sub-THz narrow band precession in metallic ferromagnets remains extremely challenging.

In the present letter, we report the results of ultrafast magneto-optical experiments with nanolayers of (Fe,Ga), i.e. Galfenol. This metallic ferromagnet with large net magnetization is considered as a prospective material for microwave spintronics due to the narrow ferromagnetic resonance [19, 20] and enhanced magnetostriction [21], which allows manipulation of the magnetization direction and precession frequency by applying stress, i.e. without changing the external magnetic field [19, 22]. Our study extends significantly the application potential of Galfenol. We show that in a Galfenol layer with a thickness of several nanometers, the femtosecond optical excitation leads to the generation of single-mode magnetization precession with frequency $f > 100$ GHz and large amplitude. Despite the strong interaction between the magnetization and the lattice, we observe a weak damping of precession with $\alpha_{eff} \approx 0.005$. Thus, we demonstrate the possibility to achieve the desirable combination of sub-THz magnetization precession with large amplitude and tunable narrow spectral band. Moreover, we

show that, depending on the nanolayer thickness, we can excite multi- or single-mode magnetization precession: in a thick 120-nm Galfenol layer we observe multimode precession and resolve up to 6 precessional localized magnon modes. This allows control of the precession spectral content and spatial profile by adjusting the film thickness and excitation regime.

The samples studied are four $Fe_{0.81}Ga_{0.19}$ nanolayers with thicknesses d= 4, 5, 20 and 120 nm grown by magnetron sputtering on (001) semi-insulating GaAs substrates and covered by a 3-nm cap layer of Al (4-nm $Fe_{0.81}Ga_{0.19}$ layer) or Cr (other nanolayers) to prevent oxidation. A 150-nm thick SiO_2 cap was deposited on the Galfenol nanolayers with a thickness $\leq$20 nm for amplification of the magnetooptical Kerr effect [23]. Room temperature experiments were carried out with an external magnetic field **B** applied in the layer plane. The in-plane direction of **B** is defined by the azimuthal angle φ_B [see the schematic in Fig. 1(a)]. In all studied layers the easy axes of magnetization are in the layer plane and close to the [100]/[010] crystallographic directions, while the hard axes are along the [110] and [1$\bar{1}$0] diagonals. All nanolayers possess a weak uniaxial in-plane anisotropy, which is typical for thin Galfenol films on GaAs substrates [22]. We have checked that the SiO_2 cap does not affect the anisotropy parameters of the layers.

The magnetization precession was excited by 150-fs pump pulses from a mode-locked Erbium-doped ring fiber laser (80 MHz repetition rate, 1050 nm wavelength). The pump beam, focused to a spot of 20 μm diameter with an energy density of $\approx$ 1 mJ/cm^2, launched the magnetization precession by ultrafast changes of the magnetic anisotropy altered by the optically-induced heating [24]. The magnetization response was monitored using 150-fs linearly polarized probe pulses of 780-nm wavelength from another ring-fiber laser oscillator focused to a 5μm spot in the center of the pump beam. For monitoring the time evolution of the magnetization precession, we utilized the transient polar magneto-optical Kerr effect (TPMOKE) and detected the rotation of the polarization of the probe beam reflected from the (Fe,Ga) layer by means of a differential scheme based on a balanced photoreceiver. In the used detection scheme the signal is proportional to the changes of the magnetization projection ΔM_z, where z is the normal to the (Fe,Ga) layer. Simultaneously by monitoring the signal from a single photodiode of a balanced photoreceiver, we measured the intensity modulation of the probe pulse, $\Delta I(t)$. The temporal resolution was achieved by means of an Asynchronous Optical Sampling System (ASOPS) [25]. The pump and probe oscillators were locked with a frequency offset of 800 Hz. In combination with the 80-MHz repetition rate, it allows measurement of the time-resolved signal in a time window of 12.5 ns with time resolution limited by the probe pulse duration.

For the measurements at magnetic fields $B > 1$ T, the samples were mounted in an optical cryostat with a superconducting solenoid. In this case, the temperature of the sample was 150 K. The source of the laser pulses was a regenerative amplifier RegA (wavelength 800 nm, repetition rate 100 kHz) and a standard scanning delay line was used to monitor the temporal evolution of the magnetization.

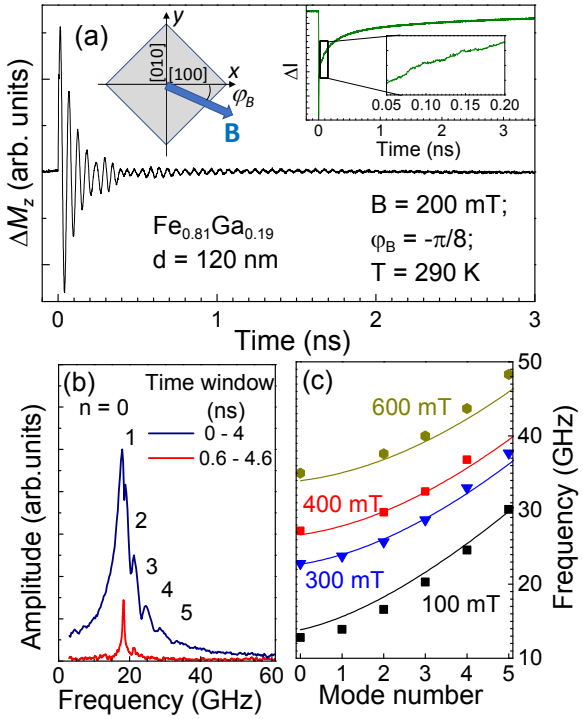

FIG. 1. Multimode magnon excitation; $T = 290$ K. (a) Temporal evolution of the magnetization precession (main panel) and modulation of the probe pulse intensity $\Delta I(t)$ (right inset) in a 120-nm thick $Fe_{0.81}Ga_{0.19}$ layer. The schematic in the left inset shows the in-plane magnetic field configuration. (b) Fast Fourier transform of the TPMOKE signal shown in (a) performed in a time window of 4 ns, with the start point at $t = 0$ (blue curve) and $t = 0.6$ ns (red curve); vertical bars point at the frequency of resonance modes with $n = 0, 1, 2, 3 \ldots$(c) Measured (symbols) and calculated (lines) dependences of resonance frequency on the mode number for several in-plane magnetic fields.

Figure 1 shows the experimental results for the thickest $d = 120$ nm $Fe_{0.81}Ga_{0.19}$ layer obtained at $\varphi_B = -\pi/8$, when the precession amplitude is maximal. The inset in Fig. 1(a) shows the signal $\Delta I(t)$, which demonstrates a rapid decrease of the reflectivity at $t = 0$ due to the optical excitation of the electron gas in the metallic galfenol layer accompanied by permittivity changes. The energy passed from hot electrons to the lattice within several picoseconds [26] leads to an increase of the lattice temperature and to a modification of the magnetic anisotropy [24]. This launches the magnetization precession, which is monitored by the TPMOKE signal and shown in the main panel of Fig. 1(a). The magnetization precession

decays in a time much less than 1 ns, which is consistent with the result for (Fe,Ga) films reported earlier [24, 27]. However, in contrast with the previous experiments, temporal beatings with a long-living tail are clearly observed. The fast Fourier transform (FFT) of the measured signal obtained in a time window of 4 ns is shown in Fig. 1(b). The blue line possesses a band spectrum where overlapping peaks are marked by integer numbers. Six spectral bands with frequencies $f_n (n = 0 \ldots 5)$ are recognized in the spectrum. We attribute these bands to standing spin wave (magnon) modes. This conclusion is based on a comparison of the experimental dependence of f_n on n, shown in Fig. 1(c) by symbols, with the well-known dispersion relation for magnon modes [28, 29]:

$$f_n - f_0 \propto \beta(B) D q_n^2, \qquad (1)$$

where q_n is the wavevector of the mode $n = 0, 1, 2, 3 \ldots$, D is the exchange spin stiffness, and β is a field dependent coefficient determined by the anisotropy parameters of the ferromagnet. The detailed analysis of the data shown in Fig. 1(c) in combination with the azimuthal dependence $f_0(B)$ can be found in the Supplemental Material [30]. The best fit of the experimental data shown by solid curves in Fig. 1(c) is obtained for the pinning boundary conditions [$q_n = \pi(n + 1)/d$], which are reasonable for an iron-based ferromagnetic film grown on GaAs [31] and covered by a 3d antiferromagnetic metal (Cr) [32]. The respective value of $D = 1.5 \times 10^{-17}$ Tm^2 (21 pJ/m) is in perfect agreement with the spin stiffness coefficient measured for Galfenol in the FMR experiment [33].

It is interesting that the FFT obtained in a temporal window which starts 600 ps after the pump pulse [red line in Fig. 1(b)] shows only two spectral lines with frequencies corresponding to $n = 0$ and 2. We may conclude that different magnon modes have different decay times and that modes with uneven n decay more quickly than modes with even n. The explanation of such behavior is related to the magnon decay mechanisms which are widely discussed in the literature [9] but still not fully understood. Two-magnon scattering [34] and the related selection rules could be the explanation, but this requires a comprehensive theoretical study which is beyond the scope of the present work.

The precession kinetics change drastically in thin nanolayers with $d = 4$, 5 and 20 nm. Figure 2 shows the temporal evolutions (left panels) and their FFTs (right panels) of magnetization precession measured for $B = 200$ mT applied at $\varphi_B = -\pi/8$. Only one spectral line is observed in the magnon spectrum, which corresponds to the fundamental mode with $n = 0$. The precession damping is well described with a single exponential decay with constants $\tau = 1.05$, 0.85, and 0.6 ns, which correspond to $\alpha_{eff} = 0.008$, 0.01 and 0.014 for the 4, 5, and 20-nm layers, respectively. The intensity signals measured in these three nanolayers also differ from the signal measured in the layer of 120-nm thickness. The inset in Fig. 2(c) shows $\Delta I(t)$ measured in the thinnest 4-nm nanolayer simultaneously with the TPMOKE signal shown in the main panel. It demonstrates an instant decrease of $\Delta I(t)$ at $t = 0$ with the subsequent slow recovery as for the 120-nm layer, but possesses pronounced oscillations with frequency $f = 44$ GHz, which is independent of the external magnetic field. These oscillations are due to dynamical interference induced by reflection of the probe pulse at the picosecond strain pulse generated in the Galfenol layer and propagating in the GaAs substrate [35], the so-called dynamical Brillouin oscillations.

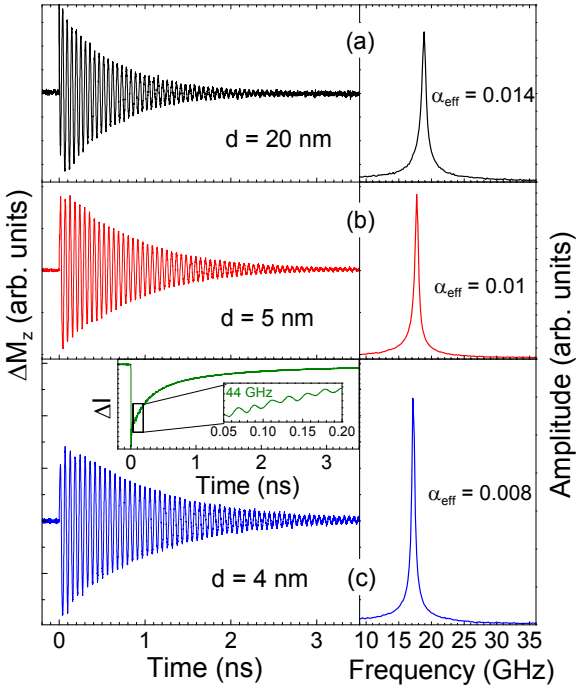

FIG. 2. Single-mode magnon excitation; $T = 290$ K. Temporal evolutions (left panels) and corresponding spectra (right panels) of the magnetization precession for $Fe_{0.81}Ga_{0.19}$ layers with different thickness measured at $B = 200$ mT and $\varphi_B = -\pi/8$. The inset in (c) shows the $\Delta I(t)$ signal measured in the 4-nm layer at the same experimental conditions.

Figure 3 shows the field dependences of the main parameters of the magnetization precession in the thinnest 4-nm layer. The precession frequency gradually increases with magnetic field [Fig 3(a)], while the precession amplitude in contrast decreases with the increase of B [Fig. 3(b)]. However, the optically excited magnetization precession remains easily detectable, even at high magnetic fields. Figure 3(c) shows the TPMOKE signal measured in the 4-nm layer at B=3 T by means of the RegA setup. The precession frequency is $f = 108$ GHz, which corresponds to the maximum precession frequency in the present work. The FFT spectrum shown in the inset of Fig. 3(c) contains also a Brillouin line at 44 GHz. The presence of this frequency in the spectrum of the

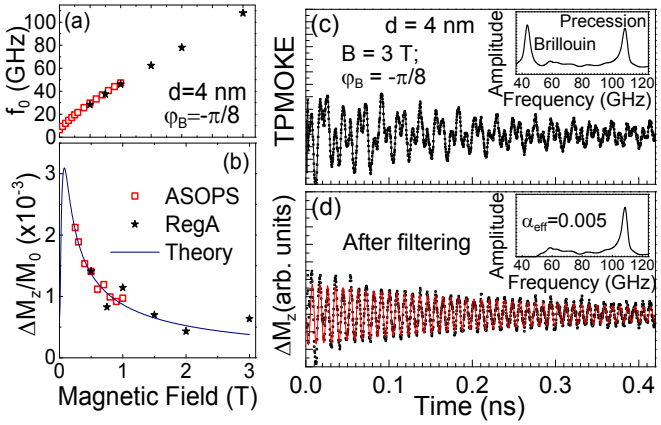

FIG. 3. (a),(b) Dependences of the frequency (a) and normalized amplitude (b) of the magnetization precession in the 4-nm thick $Fe_{0.81}Ga_{0.19}$ nanolayer; squares and stars correspond to the data measured by the ASOPS system and by scanning delay line with excitation by the RegA, respectively. Solid line in (b) shows the dependences calculated in accordance with Eq (3). (c) TPMOKE signal and its FFT spectrum (inset) measured in the 4-nm thick $Fe_{0.81}Ga_{0.19}$ nanolayer at B = 3 T and T = 150 K: (d) Temporal evolution of the magnetization precession obtained by high-pass filtering of the signal in (c): dots - experimental data; red line - fit with a single-frequency decaying sine function; inset is the corresponding FFT spectrum;

TPMOKE signal is due to imperfect balancing of a photoreceiver at the low repetition rate of a regenerative amplifier, when the single laser pulses should be balanced. Single mode excitation is observed for the filtered signal (high-pass filter with 50 GHz cutoff frequency) shown in Fig. 3(d). The decay time of the magnetization precession in the 4-nm layer at $f = 108$ GHz is $\tau = 0.29$ ns, which corresponds to an effective damping parameter $\alpha_{eff} = 0.005$.

The line in Fig. 3(d) is a fit to the experimental data by an exponentially decaying sine function:

$$\Delta M_z = A \exp(-t/\tau) \sin(\omega t + \psi), \qquad (2)$$

where $\omega = 2\pi f$ (f is obtained from the FFT spectrum). The fitting parameters A, τ, and ψ are the amplitude, decay time and the initial precession phase, respectively. The dependence of the amplitude, A on B for the thinnest (Fe,Ga) nanolayer is shown by symbols in Fig. 3(b). It is seen that A decreases with increasing B, but in our experiment it is still possible to detect the precession with frequency higher than 100 GHz at $B = 3$ T.

The main experimental results of the present work are the demonstration of excitation of a multimode quantized precession spectrum in a thick, 120-nm, (Fe,Ga) layer, and a long-living single mode magnetization precession with a frequency > 100 GHz in a thin, 4-nm, (Fe,Ga) nanolayer. Our qualitative explanation for these experimental facts is based on a comparison of the optical penetration depth in (Fe,Ga) with the layer thickness, d. The penetration depth for the pump light is $\eta \approx 20$ nm, which is larger than the thickness of the films where only one magnon mode is excited. This is confirmed by detection of the Brillouin oscillations in $\Delta I(t)$ and, thus, partial transparency of the thin galfenol layer for the probe light, which is assumed to have the same penetration depth as the pump pulse. In this case, the optical excitation, which kicks the magnetization precession, is almost homogeneous along the thickness of the nanolayer. This results in the excitation of only the ground magnon mode, while the higher order magnon modes are not excited due to their sign-changing spatial profile [7]. In contrast, in thick films $\eta < d$, and the excitation is inhomogeneous, being stronger near the surface, resulting in the efficient excitation of high-energy magnon modes. The efficiency of such excitation should decrease with the increase of n, which is clearly observed in Fig. 1(b): the spectral amplitude of the magnon spectral line decreases by more than one order of magnitude with n increasing from 0 to 5. It is important to note that due to the shallow penetration depth of the probe pulse, both even and odd magnon modes contribute to the TPMOKE signal and we see monotonic decrease of the magnon mode amplitude with increase of its number.

We now consider the observation of precession with frequency ≈ 100 GHz. Fitting the measured temporal signal shown in Fig. 3(b) with a single harmonic function gives a decay τ=0.29 ns and a respective value for $\alpha_{eff} = 0.005$. This value is close to the smallest damping parameters measured in pure Fe on semiconductor substrates by the FMR technique [36–39], but has not been reported in experiments using ultrafast optical excitation of the magnetization precession in metallic ferromagnetic materials so far.

We have performed a theoretical analysis of the precessional response of the magnetization and its dependence on magnetic field strength and direction using the approach presented in earlier work [24], which considers launching of the magnetization precession by ultrafast modification of the magnetic anisotropy. The comprehensive study of the angular dependences $f(\varphi_B)$ and $A(\varphi_B, B)$, which can be found in the Supplemental Material [30], allows us to obtain the main parameters of the 4-nm layer: saturation magnetization $\mu_0 M_0 = 1.72$ T, cubic anisotropy coefficient $K_1 = 15$ mT and uniaxial anisotropy coefficient $K_u = 5$ mT. We also confirmed experimentally that for the used pump excitation density, the demagnetization is negligible [30]. The optically-induced changes of the anisotropy coefficients were estimated by using the data from Ref. [24]: $\Delta K_1 = -3.7$ mT and $\Delta K_u = -0.8$ mT. The respective dependence of the precession amplitude on magnetic field calculated at $\varphi_B = -\pi/8$ is shown by the solid line in Fig. 3(b). A good agreement between the experimental dependence, which is normalized accordingly, and the the-

oretical curve is clearly observed. Moreover, for relatively small changes of the anisotropy coefficients, and neglecting demagnetization, we can simplify the dependence $A(\varphi_B, B)$ to:

$$A \approx \frac{(\Delta K_1/2)\sin 4\varphi_B - \Delta K_u \cos 2\varphi_B}{\sqrt{B(B+\mu_0 M_0)}}. \qquad (3)$$

This expression is valid with high accuracy at $B \geq 200$ mT. As one can see from Eq.(3), the precession amplitude is maximal at $\varphi_B = -\pi/8$ ($-3\pi/8$, $5\pi/8$, and $7\pi/8$), and remains nonzero with increase of magnetic field due to the field-independent ΔK_1 and ΔK_u. At $B = 9$ T, when the precession frequency approaches the terahertz range ($f = 300$ GHz), the estimated precession amplitude $\Delta M_z/M_0 = 3 \times 10^{-4}$ is expected to be easily detectable.

It is worth noting that in the 4-nm layer α_{eff} demonstrates a pronounced angular dependence and is 1.5 times smaller at $\varphi_B = \pi/4$ than at $\varphi_B = -\pi/8$ [30]. Unfortunately, the small precession amplitude at $\mathbf{B} \parallel [110]$ does not allow us to detect the magnetization precession at high magnetic fields applied along this direction. The angular dependence of α_{eff} may be attributed to the anisotropic Gilbert damping, which has been previously observed in Fe nanolayers and is actively studied nowadays [37–39]. The angular dependence of the Gilbert damping coefficient obtained from $\alpha_{eff}(\varphi_B)$ confirms this assumption [30].

In conclusion, we have demonstrated multimode excitation of magnetization precession in $Fe_{0.81}Ga_{0.19}$ layers with a thickness of 120 nm and single-mode precession in thin $Fe_{0.81}Ga_{0.19}$ nanolayers. We show that the parameters of (Fe,Ga) provide the possibility to detect magnetization precession with frequency higher than 100 GHz, and small effective damping parameter $\alpha_{eff} \approx 0.005$. These are record values for experiments using optical excitation of magnetization precession in metallic ferromagnets. In combination with the high responsiveness to optical excitation, this makes galfenol a prospective material for ultrafast photo-magnonics, which utilizes spatially-localized femtosecond optical excitation for the generation of propagating spin waves [40–42]. Due to the large saturation magnetization, the precession amplitude of $10^{-3}M_0$ observed at high magnetic fields generates an ac-induction of 1 mT, which may be exploited for nanoscale generators of microwave magnetic field [43] and pure spin currents [44]. Our analysis shows that 100 GHz is not the limit for the detectable magnetization precession and the THz range can be achieved by applying an appropriate external magnetic field.

ACKNOWLEDGEMENTS

We are grateful to Serhii Kukhtaruk and Alexandra Kalashnikova for fruitful discussions. This work was supported by the Deutsche Forschungsgemeinschaft and the Russian Foundation for Basic Research in the frame of the International Collaborative Research Center TRR160 [project B6] and by the Bundesministerium für Bildung und Forschung through the project VIP+ "Nanomagnetron". The experimental studies in the Laboratory of Physics of Ferroics (Ioffe Institute) were performed under support of the Russian Science Foundation [grant no. 16-12-10485]. The Volkswagen Foundation supported the cooperation with the Lashkarev Institute [grant no. 90418].

[1] J.-G. Zhu, X. Zhu, Y. Tang, IEEE Trans. Magn. **44**, 125 (2008).
[2] T. Chen, R. K. Dumas, A. Eklund, P. K. Muduli, A. Houshang, A. A. Awad, P. Dürrenfeld, B. G. Malm, A. Rusu, and J. Åkerman, IEEE Proc. **104**, 1919 (2016).
[3] A. V. Chumak, V. I. Vasyuchka, A. A. Serga, and B. Hillebrands, Nat. Phys. **11**, 453 (2015).
[4] M. Althammer, M. Weiler, H. Huebl, and S.T.B. Goennenwein, in *Spintronics for Next Generation Innovative Devices*, edited by K. Sato and E. Saitoh (Wiley, Haboken (NJ) 2016), p.111.
[5] S. I. Kiselev, J. C. Sankey, I. N. Krivorotov, N. C. Emley, R. J. Schoelkopf, R. A. Buhrman, and D. C. Ralph, Nature **425**, 380 (2003).
[6] W. K. Hiebert, A. Stankiewicz, and M. R. Freeman, Phys. Rev. Lett. **79**, 1134 (1997).
[7] M. van Kampen, C. Jozsa, J. T. Kohlhepp, P. Le Clair, L. Lagae, W. J. M. de Jonge, and B. Koopmans, Phys. Rev. Lett. **88**, 227201 (2002).
[8] A. V. Scherbakov, A.S. Salasyuk, A.V. Akimov, X. Liu, M. Bombeck, C. Bruggemann, D.R. Yakovlev, V.F. Sapega, J.K. Furdyna, and M. Bayer, Phys. Rev. Lett. **105**, 117204 (2010).
[9] A. Barman and J. Sinha, *Spin Dynamics and Damping in Ferromagnetic Thin Films and Nanostructures* (Springer, 2018), p.83
[10] A. V. Kimel, A. Kirilyuk, P. A. Usachev, R. V. Pisarev, A. M. Balbashov, and Th. Rasing, Nature **435**, 655 (2005).
[11] S. Mizukami, F. Wu, A. Sakuma, J. Walowski, D. Watanabe, T. Kubota, X. Zhang, H. Naganuma, M. Oogane, Y. Ando, and T. Miyazaki, Phys. Rev. Lett. **106**, 117201 (2011).
[12] H. B. Zhao, D. Talbayev, Q. G. Yang, G. Lüpkea, A. T. Hanbicki, C. H. Li, O. M. J. van 't Erve, G. Kioseoglou, and B. T. Jonker, Appl. Phys. Lett. **86**, 152512 (2005).
[13] M. Vomir, L. H. F. Andrade, L. Guidoni, E. Beaurepaire, and J.-Y.Bigot, Phys. Rev. Lett. **94**, 237601 (2005).
[14] J.-Y. Bigot, M. Vomir, L.H.F. Andrade, and E. Beaurepaire, J. Chem. Phys. **318**, 137 (2005).
[15] A. A. Rzhevsky, B. B. Krichevtsov, D. E. Bürgler, and C. M. Schneider, Phys. Rev. B **75**, 224434 (2007).

[16] E. Carpene, E. Mancini, D. Dazzi, C. Dallera, E. Puppin, and S. De Silvestri, Phys. Rev. B **81**, 060415 (2010).

[17] S. Mizukami, E. P. Sajitha, D. Watanabe, F. Wu, T. Miyazaki, H. Naganuma, M. Oogane, and Y. Ando, Appl. Phys. Lett. **96**, 152502 (2010).

[18] J. Kisielewski, A. Kirilyuk, A. Stupakiewicz, A. Maziewski, A. Kimel, Th. Rasing, L. T. Baczewski, and A. Wawro, Phys. Rev. B **85**, 184429 (2012).

[19] D. E. Parkes, L. R. Shelford, P. Wadley, V. Holý, M. Wang, A. T. Hindmarch, G. van der Laan, R. P. Campion, K. W. Edmonds, S. A. Cavill, and A. W. Rushforth, Sci. Reports **3**, 2220 (2013).

[20] B. K. Kuanr, R. E. Camley, Z. Celinski, A. McClure, and Y. Idzerda, J. Appl. Phys, **115**, 17C112 (2014).

[21] J. Atulasimha and A. B. Flatau, Smart Mater. Struct. **20**, 043001 (2011).

[22] D. E. Parkes, S. A. Cavill, A. T. Hindmarch, P. Wadley, F. McGee, C. R. Staddon, K. W. Edmonds, R. P. Campion, B. L. Gallagher, and A. W. Rushforth, Appl. Phys. Lett.**101**, 072402 (2012).

[23] A.V. Sokolov, *Optical Properties of Metals* (Blackie: London, 1967). p 311.

[24] V. N. Kats, T. L. Linnik, A. S. Salasyuk, A. W. Rushforth, M. Wang, P. Wadley, A. V. Akimov, S. A. Cavill, V. Holy, A. M. Kalashnikova, and A. V. Scherbakov, Phys. Rev. B **93**, 214422 (2016).

[25] A. Bartels, R. Cerna, C. Kistner, A. Thoma, F. Hudert, C. Janke, and T. Dekorsy, Rev. Sci. Instrum. **78**, 035107 (2007).

[26] G. Tas and H. J. Maris, Phys. Rev. B **49**, 15046 (1994).

[27] J. V. Jäger, A. V. Scherbakov, T. L. Linnik, D. R. Yakovlev, M. Wang, P. Wadley, V. Holy, S. A. Cavill, A. V. Akimov, A. W. Rushforth, and M. Bayer, Appl. Phys. Lett. **103**, 032409 (2013).

[28] A. G. Gurevich, G. A. Melkov, *Magnetization Oscillations and Waves* (CRC-Press, Boca Raton, 1996).

[29] S. Shihab, H. Riahi, L. Thevenard, H.J.von Bardeleben, A.Lemaitre, and C. Gourdon, Appl. Phys. Lett. **106**, 142408 (2015).

[30] See Supplemental Material at http://...

[31] Y. Fan, H. B. Zhao, G. Lupke, A. T. Hanbicki, C. H. Li, and B. T. Jonker, Phys. Rev. B **85**, 165311 (2012).

[32] P. Pincus, Phys. Rev. **118**, 658 (1960).

[33] D. B. Gopman, V. Sampath, H. Ahmad, S. Bandyopadhyay, and J. Atulasimha, IEEE Trans Magn. **53**, 6101304 (2017).

[34] R. Arias and D. L. Mills, Phys Rev B **60**, 7395 (1999)

[35] C. Thomsen, H. T. Grahn, H. J. Maris, and J. Tauc, Opt. Commun. **60**, 55 (1986).

[36] R. Urban, B. Heinrich, G. Woltersdorf, K. Ajdari, K. Myrtle, J. F. Cochran, and E. Rozenberg, Phys. Rev. B **65**, 020402(R) (2001).

[37] R. Meckenstocka, D. Spoddiga, Z. Fraitb, V. Kamberskyb, J. Pelzla, J. Mag. Mag. Mat. **272**–**276**, 1203 (2004).

[38] Y. Zhai, C. Ni, Y. Xu, Y. B. Xu, J. Wu, H. X. Lu, and H. R. Zhai, J. Appl. Phys. **101**, 09D120 (2007).

[39] L. Chen, S. Mankovsky, S. Wimmer, M. A. W. Schoen, H. S. Körner, M. Kronseder, D. Schuh, D. Bougeard, H. Ebert, D. Weiss and C. H. Back, Nat. Phys. **14**, 490 (2018).

[40] T. Satoh, Y. Terui, R. Moriya, B. A. Ivanov, K. Ando, E. Saitoh, T. Shimura, and K. Kuroda, Nat. Photonics **6**, 662 (2012).

[41] Y. Au, M. Dvornik, T. Davison, E. Ahmad, P. S. Keatley, A. Vansteenkiste, B. Van Waeyenberge, and V. V. Kruglyak, Phys. Rev. Lett. **110**, 097201 (2013).

[42] S. Iihama, Y. Sasaki, A. Sugihara, A. Kamimaki, Y. Ando, and S. Mizukami Phys. Rev. B **94**, 020401(R) (2016).

[43] A. S. Salasyuk, A. V. Rudkovskaya, A. P. Danilov, B. A. Glavin, S. M. Kukhtaruk, M. Wang, A. W. Rushforth, P. A. Nekludova, S. V. Sokolov, A. A. Elistratov, D. R. Yakovlev, M. Bayer, A. V. Akimov, and A. V. Scherbakov, Phys. Rev. B **97**, 060404(R) (2018).

[44] A. P. Danilov, A. V. Scherbakov, B. A. Glavin, T. L. Linnik, A. M. Kalashnikova, L. A. Shelukhin, D. P. Pattnaik, A. W. Rushforth, C. J. Love, S. A. Cavill, D. R. Yakovlev, and M. Bayer, Phys. Rev. B **98**, 060406(R) (2018).